Available online at www.sciencedirect.com
ScienceDirect
International Journal of Heat and Mass Transfer 50 (2007) 3115–3121
International Journal of HEAT and MASS TRANSFER
www.elsevier.com/locate/ijhmt

Characterization of electroosmotic flow in rectangular microchannels

Cheng Wang, Teck Neng Wong *, Chun Yang, Kim Tiow Ooi

School of Mechanical and Aerospace Engineering, Nanyang Technological University, Nanyang Avenue 50, Singapore 639798, Singapore

Received 5 August 2005; received in revised form 18 July 2006
Available online 22 February 2007

Abstract

In this paper, the electroosmotic displacing process between two solutions (namely the same electrolyte of different concentrations) in a rectangular microchannel is studied theoretically and experimentally. Firstly, the electric potential and velocity field in a rectangular microchannel are obtained by solving the governing equations. Fourier transform method is used to solve the electrolyte concentration profile equation. The electric current versus time curve through the microchannel is predicted based on the concentration profile obtained. The current monitoring technique is then used to study the electroosmotic displacing process. The results from the measured current–time relations agree well with those from the prediction, suggesting a reliable theoretical model developed in this study.

Keywords: Theoretical model; Electroosmotic; Rectangular microchannel; Solution displacement

1. Introduction

The study in microfluidics is rapidly becoming a very important area of research due to numerous potential applications in separation and analysis. Performing biological analysis on a microfluidics based bioMEMS or lab-on-a-chip usually involves sample preparation, treatment, injection, delivery, separation and detection. Most substances acquire surface electric charges when in contact with an aqueous (polar) medium. The rearrangement of the charges on the solid surface and the balancing charges in the liquid results in the formation of the electrical double layer (EDL) [1]. If an electric field is applied tangentially along a charged surface, the electric field will exert a body force on the ions in the diffuse layer, resulting in electroosmotic flow (EOF). EOF can provide a very flat velocity profile, thus avoiding smearing [2]. Besides, other advantages of electroosmotic pumping such as valve-less switching, accurate control of transportation and manipulation of liquid sample by an electrical field and with no solid moving parts make electroosmosis a preferred method for transporting liquids in microfluidics.

Burgreen and Nakache [3] studied the effect of the surface potential on liquid transport through ultrafine capillary slits assuming Debye–Hückel linear approximation for the electrical potential distribution under an imposed electrical field. Rice and White [4] discussed the same problem in narrow cylindrical capillaries. Levine et al. [5] extended the Rice and Whitehead's model to cases involving high zeta potentials. Yang and Li [6] studied the electrokinetic effects of pressure-driven flow in rectangular microchannels using a finite difference scheme. In Yang's study, the motion of the liquid with electrokinetic effects was analytically solved by employing the Green function formulation. Mala et al. [7] reported a study of microchannel flow and heat transfer in two parallel plates. Tsao [8] studied the electroosmosis through an annulus with Debye–Hückel linear approximation and Kang et al. [9] studied the electroosmosis in annuli with high zeta potentials by introducing a correction to account for the finite thickness of the EDL and geometrically related factors. More recently, the alternating current (AC) electroosmosis in rectangular microchannels has been studied by Yang et al. [10], Erickson and Li [11], and Marcos et al. [12].

* Corresponding author. Tel.: +65 67905877; fax: +65 67911895.
E-mail address: mtnwong@ntu.edu.sg (T.N. Wong).

0017-9310/$ - see front matter © 2007 Elsevier Ltd. All rights reserved.
doi:10.1016/j.ijheatmasstransfer.2006.11.035

In applications, electroosmotic pumps have been fabricated by packing micron sized particles into fused silica capillaries [13] and by using standard micromachining techniques [14].

In studying the electrokinetic phenomena, one of the most important characterization parameters is zeta potential. In many practical situations, it is difficult to obtain a reliable estimate of zeta potential, because zeta potential cannot be measured directly. Different ways to measure the value of zeta potential have been proposed, these include a conventional microelectrophoresis method [15] and the micro particle image velocimetry (micro-PIV) technique [16]. In the latter, Yan et al. [16] formulated an expression to determine the electrophoretic velocity of the tracer particles and the EOF field of the microchannel through the measurement of the steady velocity distributions of the tracer particles in both open- and closed-end rectangular microchannels under the same water chemical conditions. Another simple experimental method, termed the current monitoring method, was first suggested by Huang et al. [17] in which the electroosmotic flow rate was monitored using the electric current change, when one solution is electrokinetically displaced by the same solution with a slight difference in ionic concentration. Arulanandam and Li [18] employed this method to evaluate the zeta potential and the surface conductance. In these experiments, the average velocity of electroosmosis flow was determined by measuring the time required to completely displace a solution by another similar solution in the capillary tube. The zeta potential value was determined by fitting the measured average velocity to the theoretical model developed in the study [18]. Ren et al. [19] improved the current monitoring method by using the slope of the measured correlation of the current versus time to achieve a better accuracy. The electroosmotic displacing process in a circular capillary was later studied numerically by Ren et al. [20] using a finite control volume method to solve a mathematical model accounting for three zones of solution, namely solution 1 zone, mixing zone and solution 2 zone. Analytically, Ren et al. [21] developed mathematical formulations for the displacing process in the cylindrical capillaries based on two models: the sharp interface and the mixing zone models.

The above mentioned cases studied the electroosmotic flow displacing processes in cylindrical capillaries. However, in practice, the microchannel networks in lab-on-a-chip platforms are usually fabricated by microelectronic fabrication techniques [22,23], and these channels are rectangular rather than cylindrical in cross section. This paper presents an in-depth analysis of electroosmotic displacing process of one solution with another in rectangular microchannels. A mathematical model is developed to describe the electroosmotic flow in a rectangular microchannel. The model includes solving the Poisson–Boltzmann's equation for EDL potential distribution and the modified Navier–Stokes equation for the electroosmotic flow field by the separation of variables method, and the mass transport equation using Fourier transform method. Based on the mass transport equation, the average electroosmotic velocity is determined by measuring the time needed to transport the electrolyte across the microchannel. The zeta potential is also obtained. The theoretical predictions for the current–time relationship are compared with measured results. Good agreement is obtained.

2. Mathematical model

2.1. Electrical double layer potential distribution

A straight rectangular microchannel of width $2W$, height $2H$ and length L is shown in Fig. 1. In this theoretical model, the channel wall is assumed to be uniformly charged so that the electrical potential in the EDL varies in the x and y directions only. Due to the symmetry of the potential and velocity fields, the solution domain can be reduced to a quarter cross section of the channel. It is further assumed that the electric charge density is uninfluenced by the external electric field due to thin EDLs; therefore the charge convection can be ignored and thus the electric field equation and the fluid flow equation are decoupled [24]. Introducing the dimensionless parameters: $X = \frac{x}{D_h}$, $Y = \frac{y}{D_h}$, $\Psi = \frac{z_0 e}{kT}\psi$ and $D_h = \frac{4HW}{H+W}$, and assuming a small zeta potential, the electric potential due to charged wall can be described by the linearized Poisson–Boltzmann's equation which can be written in terms of dimensionless variables [12] as

$$\nabla^2 \Psi = K^2 \Psi, \tag{1}$$

where $K = \kappa D_h$ is the ratio of the length scale D_h to the characteristic double layer thickness $1/\kappa$. Here κ is the Debye–Hückel parameter, given by

$$\kappa = \left(\frac{\varepsilon_r \varepsilon_0 k_b T}{2 z_0^2 e^2 n_0}\right)^{1/2},$$

where z_0 is the valence, e is the fundamental electric charge, ψ is the electric potential, ε_r is the relative permittivity, and ε_0 is the permittivity in vacuum.

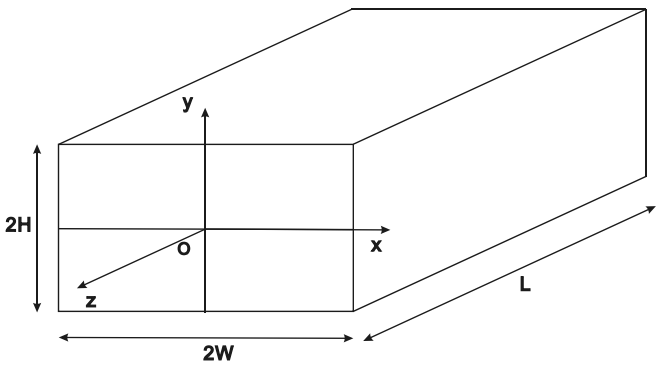

Fig. 1. Schematic of the rectangular microchannel and the coordinate system used for modeling.

The boundary conditions along the symmetrical lines is $\frac{\partial \Psi}{\partial X}=0$ at $X=0$ and $\frac{\partial \Psi}{\partial Y}=0$ at $Y=0$. At the channel wall, $\Psi=\bar{\zeta}$ at $X=\frac{W}{D_h}$ and $Y=\frac{H}{D_h}$. Using the separation of variable method, the solution to the linearized Poisson–Boltzmann equation gives

$$\begin{aligned}\Psi(X,Y)=4\bar{\zeta}\sum_{n=1}^{\infty}\frac{(-1)^{n+1}\cosh\left[\sqrt{1+\frac{(2n-1)^2\pi^2D_h^2}{4K^2W^2}}\times KY\right]}{(2n-1)\pi\cosh\left[\sqrt{1+\frac{(2n-1)^2\pi^2D_h^2}{4K^2W^2}}\times\frac{KH}{D_h}\right]}\\ \times\cos\left[\frac{(2n-1)D_h\pi}{2W}X\right]\\ +4\bar{\zeta}\sum_{m=1}^{\infty}\frac{(-1)^{m+1}\cosh\left[\sqrt{1+\frac{(2m-1)^2\pi^2D_h^2}{4K^2H^2}}\times KX\right]}{(2m-1)\pi\cosh\left[\sqrt{1+\frac{(2m-1)^2\pi^2D_h^2}{4K^2H^2}}\times\frac{KW}{D_h}\right]}\\ \times\cos\left[\frac{(2m-1)D_h\pi}{2H}Y\right].\end{aligned}\tag{2}$$

The ionic net charge density in the EDL can be expressed by [25]

$$\bar{\rho}_e=-2\Psi.\tag{3}$$

2.2. Electroosmotic flow field

The motion of an incompressible fluid is governed by the Navier–Stokes equation, which is expressed as

$$\rho\frac{\partial \mathbf{V}}{\partial t}+\rho(V\cdot\nabla)\mathbf{V}=-\nabla p+\mathbf{F}+\mu\nabla^2V,\tag{4}$$

where $\mathbf{V}$ is the velocity vector, p is the pressure, $\mathbf{F}$ is the external force, ρ and μ are the density and dynamics viscosity of the fluid [26].

Using the following assumptions

(1) The fluid is Newtonian;
(2) the properties of the fluid are independent of local electric field, thus only diluted solutions are considered in this study;
(3) the fluid's properties are temperature independent. Joule heating effect could increase the temperature, but it can be negligible for diluted solution or under low electric field strength;
(4) the flow field is steady, fully developed and obeying no-slip conditions at the channel wall, and
(5) there is no pressure gradient along the microchannel, and the two reservoirs are large enough to maintain the same pressure level.

Eq. (4) is thus reduced to

$$\mu\nabla^2u=-\rho_eE,\tag{5}$$

where E is the applied electric field strength, ρ_e is the ionic net charge density and u is the velocity [24].

The boundary conditions are described by

$$\begin{aligned}&u|_{x=W}=0,\quad u|_{y=H}=0,\\ &\left.\frac{\partial u}{\partial x}\right|_{x=0}=0,\quad \left.\frac{\partial u}{\partial y}\right|_{y=0}=0.\end{aligned}\tag{6}$$

Introducing dimensionless parameters, $U=\frac{u}{U_0}$ and using the separation of variables method, the analytical velocity field inside the quarter domain is obtained as [25,27]

$$\begin{aligned}U(X,Y)=&-4\frac{E\varepsilon_r\varepsilon_0kT}{\mu zeU_0}\bar{\zeta}\sum_{m=1}^{\infty}\frac{(-1)^{m+1}\cos\left[\frac{(2m-1)D_h\pi}{2H}Y\right]}{(2m-1)\pi}\\ &\times\left\{\frac{\cosh\left[\sqrt{1+\frac{(2m-1)^2\pi^2D_h^2}{4K^2H^2}}\times KX\right]}{\cosh\left[\sqrt{1+\frac{(2m-1)^2\pi^2D_h^2}{4K^2H^2}}\times\frac{KW}{D_h}\right]}-\frac{\cosh\left[\frac{(2m-1)D_h\pi}{2H}X\right]}{\cosh\left[\frac{(2m-1)D_h\pi}{2H}\right]}\right\}\\ &-4\frac{E\varepsilon_r\varepsilon_0kT}{\mu zeU_0}\bar{\zeta}\sum_{n=1}^{\infty}\frac{(-1)^{n+1}\cos\left[\frac{(2n-1)D_h\pi}{2W}Y\right]}{(2n-1)\pi}\\ &\times\left\{\frac{\cosh\left[\sqrt{1+\frac{(2n-1)^2\pi^2D_h^2}{4K^2W^2}}\times KY\right]}{\cosh\left[\sqrt{1+\frac{(2n-1)^2\pi^2D_h^2}{4K^2W^2}}\times\frac{KH}{D_h}\right]}-\frac{\cosh\left[\frac{(2n-1)D_h\pi}{2W}Y\right]}{\cosh\left[\frac{(2n-1)D_h\pi}{2W}\right]}\right\}.\end{aligned}\tag{7}$$

The average electroosmotic velocity can be found as

$$\overline{U}=\frac{1}{A}\int U(X,Y)\mathrm{d}A,\tag{8}$$

where the integration is over the quarter domain of the microchannel.

2.3. Solution displacement in the microchannel

The solution displacing model studied is shown in Fig. 2. There are two reservoirs containing the same electrolyte solution but with two different concentrations, c_1 and c_2, where c_1 and c_2 are not significantly different, (e.g., $c_1=70\%\ c_2$). A rectangular microchannel connects the two reservoirs. Initially, the connecting channel is filled with solution of concentration c_1. Immediately after an electric field is applied along the channel, electroosmotic flow is generated. Gradually, the solution of higher concentration from the reservoir 2 displaces the solution of lower concentration towards the reservoir 1.

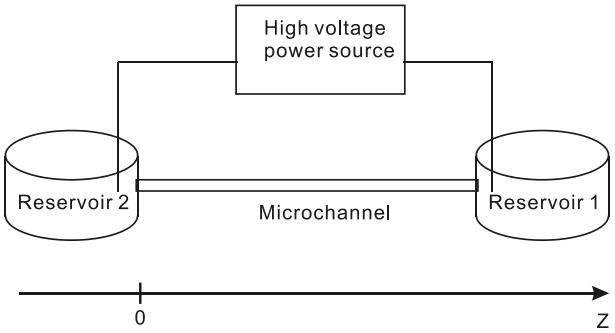

Fig. 2. Schematic of the solution displacement inside the microchannel.

The solution displacement along z direction is governed by the mass transport equation [28]

$$\frac{\partial c}{\partial t}+\bar{u}\frac{\partial c}{\partial z}=D\frac{\partial^2 c}{\partial z^2}, \tag{9}$$

where c is the bulk concentration, t is the time, $\bar{u}$ is the average velocity and D is the diffusion coefficient. By introducing non-dimensional parameters: $Pe=\frac{\bar{u}D_h}{D}$, $\bar{t}=\frac{tD}{D_h^2}$, $Z=\frac{z}{D_h}$ and $C=\frac{c-c_1}{c_2-c_1}$, Eq. (9) in the dimensionless form can be written as

$$\frac{\partial C}{\partial \bar{t}}+Pe\frac{\partial C}{\partial Z}=\frac{\partial^2 C}{\partial Z^2}, \tag{10}$$

where Pe is Peclect number. Eq. (10) is subjected to the initial and boundary conditions shown below:

$$\overline{C}|_{\bar{t}=0}=0,$$
$$\overline{C}|_{z=0}=1,$$

where $L=\frac{l}{D_h}$ is the dimensionless channel length.

Introducing new variables $\eta=Z-Pe\bar{t}$ and $\tau=\bar{t}$, the mass transport equation can be simplified to that shown in Eq. (11)

$$\frac{\partial \overline{C}}{\partial \tau}=\frac{\partial \overline{C}^2}{\partial \eta^2}. \tag{11}$$

Using the Fourier transform theorem, the Fourier transform [29] of a function $f(x)$ is

$$F(\alpha)=\frac{1}{\sqrt{2\pi}}\int_{-\infty}^{\infty} f(t)e^{i\alpha t}\,dt,$$

and the inverse Fourier transform of $F(\alpha)$ is

$$f(x)=\frac{1}{\sqrt{2\pi}}\int_{-\infty}^{\infty} F(\alpha)e^{-ixt}\,d\alpha.$$

Then, it can be shown that the solution to Eq. (11) can be expressed as

$$C(\eta,\tau)=\begin{cases}\frac{1}{2}\left[1+\operatorname{erf}\left(\frac{-\eta}{2\sqrt{\tau}}\right)\right] & \text{for } \eta<0,\\ \frac{1}{2}\left[1-\operatorname{erf}\left(\frac{\eta}{2\sqrt{\tau}}\right)\right] & \text{for } \eta>0.\end{cases} \tag{12}$$

In the z and t coordinates, Eq. (12) can be rewritten as

$$c(z,t)=\begin{cases}\frac{1}{2}(c_2-c_1)\left[1+\operatorname{erf}\left(\frac{\bar{u}t-z}{2\sqrt{Dt}}\right)\right]+c_1 & \text{for } \bar{u}t>z,\\ \frac{1}{2}(c_2-c_1)\left[1-\operatorname{erf}\left(\frac{z-\bar{u}t}{2\sqrt{Dt}}\right)\right]+c_1 & \text{for } \bar{u}t<z.\end{cases} \tag{13}$$

From the current-monitoring method, the total displacement time t_{max} can be obtained from measurement via the recorded current–time relationship, and theoretically it also satisfies $c(l,t_{max})=c_2$. Together with Eq. (13), the average velocity can be determined. Finally, the corresponding zeta potential can be found from Eqs. (7) and (8).

2.4. Current prediction

Once the concentration profile of the solution in the channel is known, the resistance of the solution and the current $I(t)$ through the channel can be found. The resistance of the solution is then given by Ohm's Law $R=\frac{l}{\lambda A_{total}}$, in which R is the resistance, l is the length, A_{total} is the total cross section area of the conductor (equals the channel cross section area), and λ is the conductivity of the electrolyte solution. Noted that λ depends on the concentration of the electrolyte solution during the solution displacement, the total resistance of the electrolyte in the channel can be written as

$$R_{total}(t)=\int_0^l \frac{dx}{\lambda_i(c)A_{total}}. \tag{14}$$

The current is given by

$$I(t)=\frac{El}{R_{total}(t)}. \tag{15}$$

3. Experimental setup and discussion

In the measurement setup, the current monitoring method is used to study the characteristics of the electroosmotic flow in a rectangular microchannel. The experimental setup consists of a high voltage power supply (CZE 1000R, Spellman, USA), a personal computer (PC), a data acquisition system (BNC 2110 unit, National Instruments Corporation), flow reservoirs (manufactured using Teflon material), and polyimide-fused silica capillaries (Polymicro Technologies Incorporated, USA).

The microcapillaries with square cross section of 100 μm × 100 μm and 75 μm × 75 μm were cut to 5 cm in length and used to connect reservoir 2 (higher concentration c_2) and reservoir 1 (lower concentration c_1). Initially, the microcapillary was filled with NaCl (Sigma–Aldrich) electrolyte solution of a lower concentration c_1. Platinum electrodes were inserted in both reservoirs with the grounding to reservoir 1 and high voltage power supply unit to reservoir 2. Measurements were conducted using electrolyte solution NaCl of different concentrations, 10^{-2} M, 10^{-3} M, in microchannel of different dimensions, 75 μm and 100 μm, under different applied electric fields of 200 V/cm, 400 V/cm, 600 V/cm and 700 V/cm.

The current–time curves from both measured and predicted are shown in Fig. 3. The electric current increases with time after an electric field is applied. An EOF is induced, whereby the higher concentration solution displaces the lower concentration one causing the variation in electrical current along the flow direction. The current reaches a constant and maximum value when the higher concentration solution completely displaces the lower concentration solution. The stable current level indicates the completion of the displacement process. The good agreement between the prediction and the measured values suggests the validation of the theoretical model.

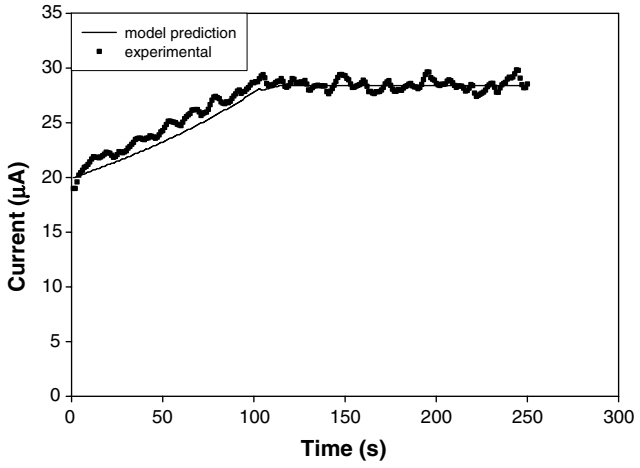

Fig. 3. Current–time curve, experimental and theoretical prediction, for NaCl 10^{-2} M, $E = 400$ V/cm, and channel of cross section of 75 μm × 75 μm.

The effects of the applied electric field strength and the ionic concentration on electroosmotic velocities are shown in Fig. 4a and b. It can be seen that the electroosmotic velocity is proportional to the applied electric field strength. The results also show that as the NaCl concentration decreases, the EOF velocity increases. Furthermore, the results show that the EOF velocity is independent of the channel size.

It is noted that the higher the NaCl concentration, the lower the zeta potential, ζ, as shown in Fig. 5. Hence the electroosmotic velocity is lower for electrolyte of higher concentration. Moreover, it is clear that ζ is independent of the electric field and channel size, suggesting that ζ is an intrinsic property of the channel material and the electrolyte solution. This is in accordance with the findings in the study of Arulanandam and Li [18].

Fig. 6 shows the variations of the dimensionless concentration profile of the solution during the displacement process. The concentration level of the solution in the microchannel can be divided into three zones, the higher concentration zone with concentration value of c_2, the lower concentration zone with concentration value of c_1 and a mixing zone with concentration value lies between c_1 and c_2. Initially, the microchannel is filled with solution with concentration value of c_1. Upon the application of an electric field, the electrolyte solution with concentration value of c_2 from reservoir 1 displaces the solution with

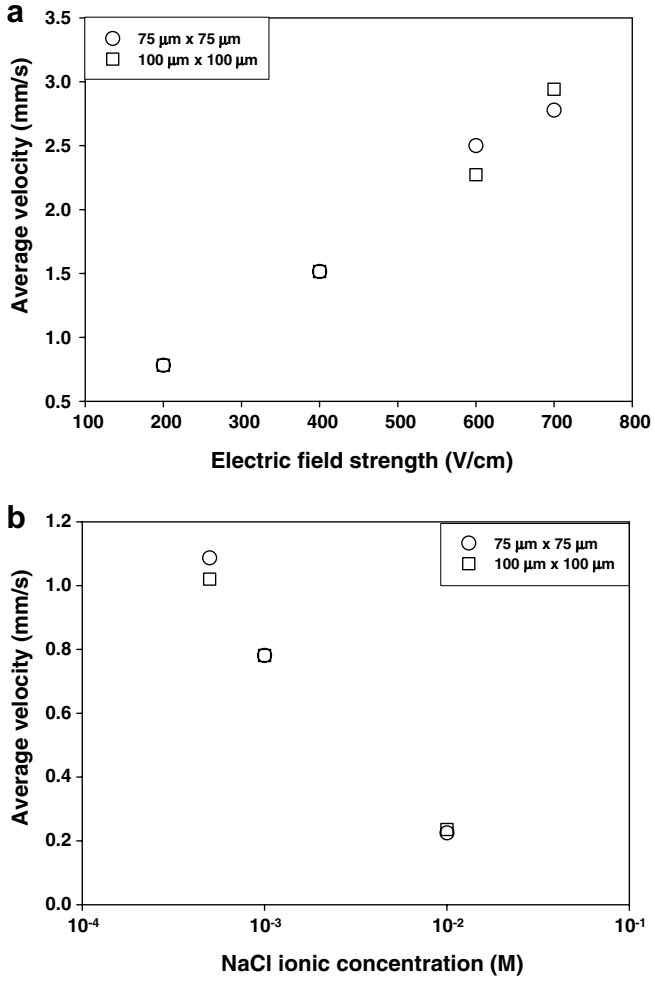

Fig. 4. Average EOF velocity versus (a) electric field strength for 10^{-3} M NaCl and (b) NaCl concentration under electric field strength 200 V/cm.

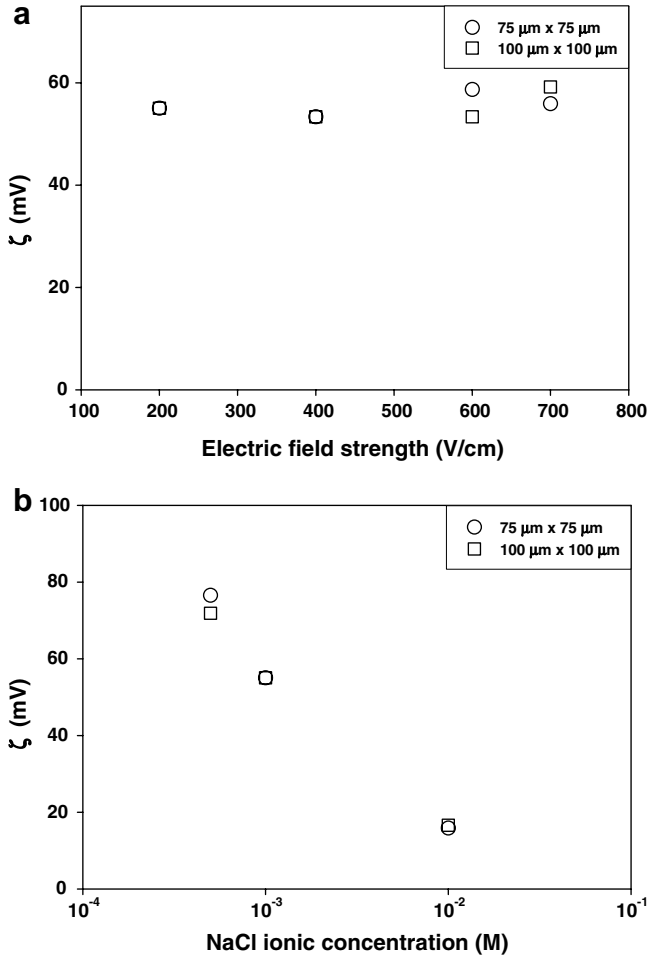

Fig. 5. ζ versus (a) electric field strength for 10^{-3} M NaCl and (b) NaCl concentration under electric field strength 200 V/cm.

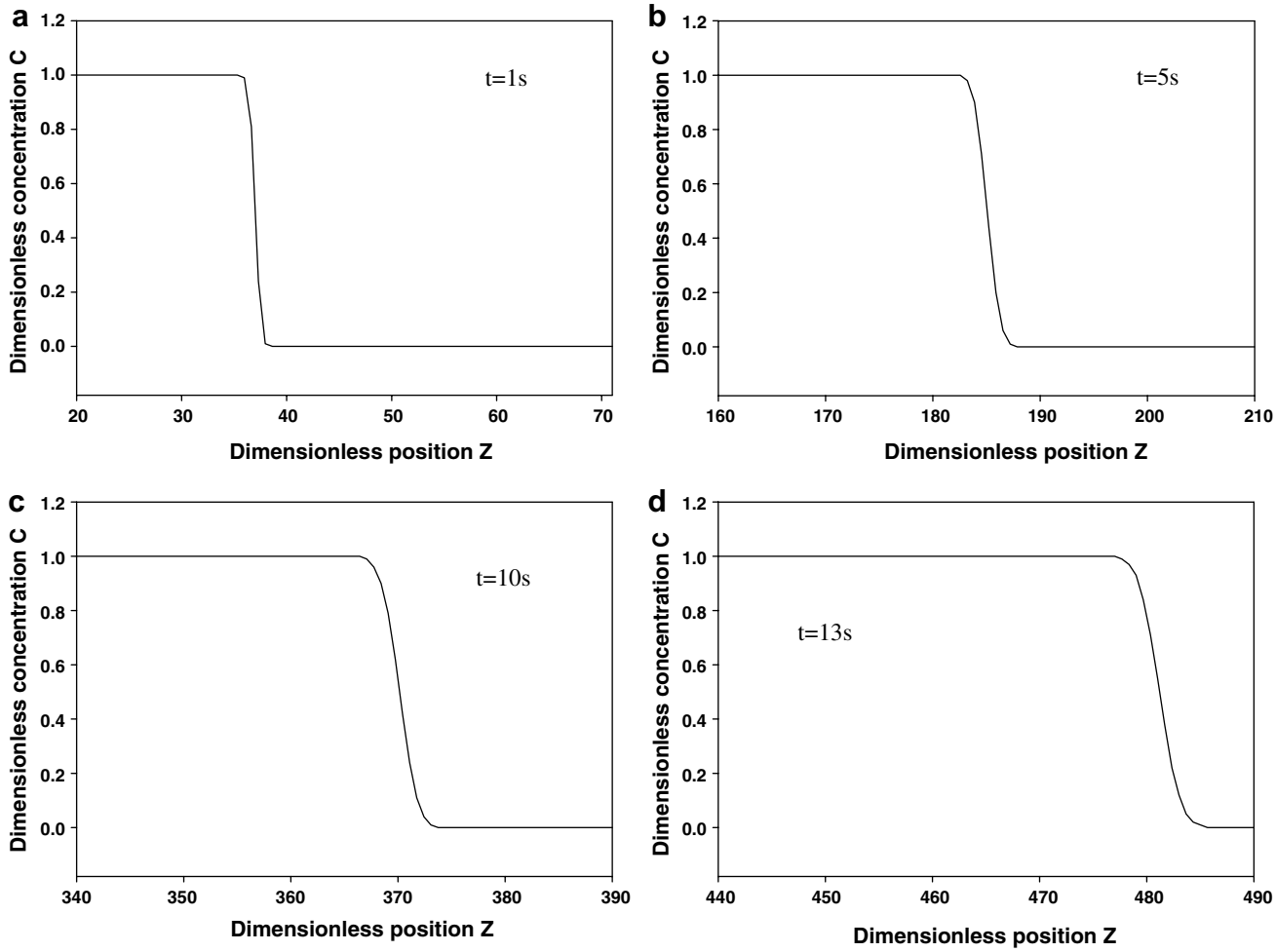

Fig. 6. Dimensionless concentration profile evolution during the displacement process, $E = 700$ V/cm, NaCl 10^{-3} M, channel with cross section of 75 μm × 75 μm: (a) at time 1 s; (b) at time 5 s; (c) at time 10 s and (d) at time 13 s.

concentration value of c_1 as a result of the electroosmotic flow. Therefore, there exists a mixing zone at the interface of these two zones.

The mixing zone becomes larger as diffusion occurs over time, as shown in Fig. 6. As compared to the total length of the microchannel, the length of the mixing zone is insignificant. Thus, in some previous work [18], a sharp interface or no mixing zone was assumed. Such assumption is reasonable only when the mixing zone length is negligible, especially in the case of short displacement time between the two solutions. However, when the EOF velocity is low as compared to the length of the channel, a longer time is needed to complete the displacement process and thus diffusion takes place over a longer time duration. In this case, the sharp interface assumption may not be accurate. In such cases, the theoretical solution proposed in this paper can better describe the displacement process.

4. Conclusion

The characteristics of electroosmotic flow in rectangular microchannels, such as electroosmotic velocity and zeta potential were investigated both theoretically and experimentally. In the theoretical analysis, the potential distribution and the velocity field of the fluid in the microchannel were derived using the Poisson–Boltzmann equation and the Navier–Stokes equation, respectively. The concentration profile of the displacement process was obtained by solving the mass transport equation using the Fourier transform method. The measured current–time relation was compared with the theoretical prediction. Good agreement between experimental results and theoretical predictions was obtained which indicates the reliability of the theoretical solution proposed in this study. The model is particularly suited for cases with non-zero mixing length between the two solutions.

References

[1] R.J. Hunter, Zeta Potential in Colloid Science: Principles and Applications, Academic Press, London, 1981, xi, 386 p.
[2] J. Knight, Honey, I shrunk the lab, Nature 418 (6897) (2002) 474–475.
[3] D. Burgreen, F.R. Nakache, Electrokinetic flow in ultrafine capillary silts, J. Phys. Chem. 68 (5) (1964) 1084–1091.

[4] C.L. Rice, R. White, Electrokinetic flow in a narrow cylindrical capillary, J. Phys. Chem. 69 (1965) 4017–4023.
[5] S. Levine et al., Theory of electrokinetic flow in fine cylindrical capillaries at high zeta-potentials, J. Colloid Interf. Sci. 52 (1975) 136–149.
[6] C. Yang, D.Q. Li, Electrokinetic effects on pressure-driven liquid flows in rectangular microchannels, J. Colloid Interf. Sci. 194 (1) (1997) 95–107.
[7] G.M. Mala, D. Li, J.D. Dale, Heat transfer and fluid flow in microchannels, Int. J. Heat Mass Transfer 40 (13) (1997) 3079–3088.
[8] H.K. Tsao, Electroosmotic flow through an annulus, J. Colloid Interf. Sci. 225 (2000) 247–250.
[9] Y. Kang, C. Yang, X. Huang, Electroosmotic flow in a capillary annulus with high zeta potentials, J. Colloid Interf. Sci. 253 (2) (2002) 285–294.
[10] J. Yang et al., Oscillating laminar electrokinetic flow in infinitely extended rectangular microchannels, J. Colloid Interf. Sci. 261 (1) (2003) 21–31.
[11] D. Erickson, D.Q. Li, Analysis of alternating current electroosmotic flows in a rectangular microchannel, Langmuir 19 (13) (2003) 5421–5430.
[12] Marcos et al., Frequency-dependent laminar electroosmotic flow in a closed-end rectangular microchannel, J. Colloid Interf. Sci. 275 (2) (2004) 679–698.
[13] S. Zeng et al., Fabrication and characterization of electrokinetic micropumps, Sens. Actuators B 79 (2001) 107–114.
[14] C.H. Chen, J.G. Santiago, A planar electroosmotic micropump, J. Microelectromech. Syst. 11 (6) (2002) 672–683.
[15] C. Yang et al., Measurement of the zeta potential of gas bubbles in aqueous solutions by microelectrophoresis method, J. Colloid Interf. Sci. 243 (2001) 128–135.
[16] D. Yan et al., A method for simultaneously determining the zeta potential of the channel surface and the tracer particles using micro-particle image velocimetry technique, Electrophoresis 27 (2006) 620–627.
[17] X. Huang, M.J. Gordan, R.N. Zare, Current-monitoring method for measuring the electroosmotic flow rate in capillary zone electrophoresis, Anal. Chem. 60 (1988) 1837–1838.
[18] S. Arulanandam, D. Li, Determining zeta potential and surface conductance by monitoring the current in electroosmotic flow, J. Colloid Interf. Sci. 225 (2000) 421–428.
[19] L.Q. Ren, C. Escobedo, D. Li, A new method of evaluating the average electro-osmotic velocity in microchannels, J. Colloid Interf. Sci. 250 (2002) 238–242.
[20] L. Ren, C. Escobedo, D. Li, Electroosmotic flow in microcapillary with one solution displacing another solution, J. Colloid Interf. Sci. 242 (2001) 264–271.
[21] L.Q. Ren, M.B. Jacob, D.Q. Li, Experimental and theoretical study of the displacement process between two electrolyte solutions in a microchannel, J. Colloid Interf. Sci. 257 (1) (2003) 85–92.
[22] N.-T. Nguyen, S.T. Wereley, Fundamentals and Applications of Microfluidics, Artech House Microelectromechanical Systems Library, Artech House, Boston, MA, 2002, xiii, 471 p.
[23] M. Koch, A. Evans, A. Brunnschweiler, Microfluidic Technology and Applications, Research Studies Press, 2000.
[24] Y. Gao et al., Two-fluid electroosmotic flow in microchannels, J. Colloid Interf. Sci. (284) (2005) 306–314.
[25] C. Yang, D.Q. Li, J.H. Masliyah, Modeling forced liquid convection in rectangular microchannels with electrokinetic effects, Int. J. Heat Mass Transfer 41 (24) (1998) 4229–4249.
[26] F.M. White, Fluid Mechanics, fourth ed., McGraw-Hill Series in Mechanical Engineering, WCB/McGraw-Hill, Boston, Mass, 1999, xiv, 825 p.
[27] C. Yang, D.Q. Li, Analysis of electrokinetic effects on the liquid flow in rectangular microchannels, Colloids Surf. A 143 (2–3) (1998) 339–353.
[28] R.B. Bird, W.E. Stewart, E.N. Lightfoot, Transport Phenomena, second ed., J. Wiley, New York, 2002, xii, 895 p.
[29] M.U. Tyn, Partial Differential Equations of Mathematical Physics, North Holland, New York, 1980.